

A Time Domain Uniform Geometrical Theory of Slope Diffraction for a Curved Wedge

Paul R. ROUSSEAU

The Aerospace Corporation., El Segundo, California, USA

Prabhakar PATHAK

The Ohio State Univ., Dept. of Electrical Enngineering, Columbus, Ohio, USA

e-mail: pathak.2@osu.edu

Abstract

A time domain version of the uniform geometrical theory of diffraction (TD-UTD) is developed to describe, in essentially closed form, the field which is produced via slope diffraction at a perfectly conducting, arbitrarily curved wedge excited by a time impulsive wave that exhibits a rapid spatial variation near the edge of the wedge. This TD-UTD slope diffracted field for a curved wedge is obtained by a Fourier inversion of the corresponding frequency domain UTD expression. An analytical signal representation of the transient fields is used since it is convenient, and because it circumvents some of the difficulties, which especially arise when inverting into time domain the frequency domain UTD fields associated with rays that have traversed caustics. The TD-UTD slope diffraction solution is obtained in a manner analogous to that utilized to develop an earlier TD-UTD solution, presented by the authors, for the case when the incident field does not exhibit a rapid spatial variation at the edge [1]. This TD-UTD slope diffraction solution for a time impulsive incident field can also be used for dealing with relatively general pulsed excitations via an efficient convolution procedure similar to that in [1]. Numerical results are presented to illustrate the accuracy of the TD-UTD solution by comparing it to the exact solution for a straight wedge with pulsed excitation, which was obtained earlier by Felsen [13].

Key Words: *time domain uniform geometrical theory of diffraction, slope diffraction, perfectly conducting curved wedge, analytical signal representation*

1. Introduction

The authors previously developed a TD-UTD solution [1] for the diffraction of a pulsed astigmatic wavefront incident on a perfectly conducting curved wedge, when the wavefront amplitude exhibits a slow spatial variation in the neighborhood of the edge. That work is extended in this paper to deal with the case when the incident wavefront exhibits a rapid spatial variation at and near the edge of the wedge. In particular, the TD-UTD wedge diffraction solution reported in [1] depends on the spatial amplitude of the pulsed incident wave at the point of diffraction on the edge. On the other hand, the TD-UTD slope wedge diffraction solution depends on the slope or the spatial derivative of the incident pulse at the point of edge diffraction and it represents a higher order correction to [1]. The more complete TD-UTD solution to the problem of transient pulse diffraction by a curved wedge must therefore be given by the sum of that in [1] and the one presented here. However, it is noted that if the spatial amplitude of the incident wave goes rapidly to zero at the point of diffraction on the edge then the diffracted field contribution to the TD-UTD solution in [1] vanishes, and only the slope diffraction contribution remains.

The motivation for this work stems from the fact that exact analytical solutions in the time domain (TD) are available only for a limited number of relatively simple configurations. On the other hand, a TD-UTD development would lead to approximate analytical wave solutions that can analyze pulse excited complex radiating/scattering objects for which exact, closed form, analytical solutions are not available. The latter is accomplished in TD in the same fashion as the UTD does for handling complex structures in the frequency domain. It is noted that the TD-UTD solutions employ the same rays as the frequency domain UTD, thus retaining the simple physical picture for radiation and scattering, which is provided by the UTD. However, the various TD rays will in general not reach the observer simultaneously as they do in the frequency domain case because of the different path lengths, which they traverse. Furthermore, the transient-field in intervals close to the arrival of each of the various significant TD-UTD ray contributions is generally the strongest, at the observer, and is directly related to the local geometrical features of the radiating/scattering object from where the rays originate. The latter is of importance to remote sensing and target identification applications. The developments in the area of ultra short pulse (or ultra wide band) radars are lending further impetus to such important applications. The study of transient radiation/scattering is also of interest in predicting the effect of both natural and man-made, electromagnetic pulses (EMPs) on complex objects such as aircraft and spacecraft. While numerical discretization methods such as the finite-difference time domain (FDTD), etc. can be utilized to analyze transient wave phenomena, they become rapidly intractable in dealing with excitation pulse widths, which are small in comparison to the overall dimension of the radiating/scattering structure. On the other hand, the TD-UTD is applicable for short pulse excitations. The accuracy of the TD-UTD is expected to decrease for late times since it is obtained by inverting into time domain the corresponding asymptotic high frequency UTD field expression. In the event that the excitation/incident pulse has a sufficiently large high frequency content and also contains relatively small low frequency components, the TD-UTD result can then remain quite accurate for early, intermediate and late times. It is noted that although the TD-UTD for a curved wedge is obtained in closed form here for the slope diffraction case, and in [1] for the ordinary diffraction case, respectively, when a time impulsive wavefront is incident on the edge, the TD-UTD response to a relatively general pulse dominated by frequencies for which the TD-UTD is accurate can be found via an efficient convolution with the impulse response. The latter convolution approach becomes efficient because it is given essentially in closed form when the general pulsed waveform can be expressed, as is true in most practical situations, in terms of a superposition of relatively few simple expansion functions which are complex exponentials in the frequency domain, together with the use of the analytic signal representation for the convolution integral as indicated in [1].

In the present development, the incident frequency domain astigmatic ray field is allowed to exhibit any polarization (e.g. linear, circular or elliptical); this incident geometrical optics (GO) field must be converted into the time domain along with the reflected GO field and the remainder diffracted and slope diffracted fields, respectively, in the construction of the complete TD-UTD solution. It is noted that the GO incident and reflected fields constitute the leading terms of any UTD solution. The present work following [1] also allows for the incident, reflected and edge diffracted rays respectively, of the UTD, to have passed through some caustics. The inversion into TD of the UTD fields, which can exhibit such relatively general properties of polarization and propagation through caustics is made more convenient with the use of the analytical signal representation for the TD fields. The analytic function is obtained from a one sided inverse Fourier transform with the time variable, t , which is allowed to be complex [1-4]. For the sake of brevity, this transform, which provides an inversion into TD of the one sided frequency (ω) domain UTD fields, to arrive at the TD-UTD, will henceforth be referred to as the analytic time transform (ATT). The work in

[2,3] by Felsen and Heyman in the area of spectral theory of transients, and also additional work by Heyman et. al. in that area [5-7], provides inspiration for the use of the analytic time representation in [1] and also in the present work. In the spectral theory of transients [2,3,5-7], an exact TD solution is developed for some canonical geometries, e.g., the straight wedge, and then approximated for early times. The TD-UTD provides an early to intermediate time pulse response directly via the ATT for more general arbitrary curved wedges and smooth convex surfaces [1,8].

Two slightly different versions of the TD-UTD for slope diffraction by a curved wedge are developed here; they are based on inverting into TD the corresponding frequency domain UTD results obtained earlier by Hwang and Kouyoumjian [9], and by Veruttipong and Kouyoumjian [10], respectively. The details of the TD-UTD development are summarized in Section 2 to follow. The two versions of the TD-UTD slope diffraction coefficients indicate slightly different levels of accuracy, and both are valid when the incident wave is rapidly varying spatially in a direction perpendicular to the incident ray at the edge. Other slope diffracted fields [11,12] are not considered in this work. In Section 3, numerical results based on the two different versions of the TD-UTD slope diffracted fields are presented and compared with an exact TD solution for the special case of a straight wedge given previously by Felsen [13]. The frequency domain UTD fields are assumed to have an $\exp(j\omega t)$ time harmonic variation, which is suppressed here.

2. Development of TD-UTD for Slope Wedge Diffraction

The general solution for the TD-UTD electric field in the case of a perfectly conducting curved wedge, when illuminated by an external time impulsive astigmatic wavefront, can be expressed as

$${}^{+UTD}\mathbf{E}_I(t) = \mathbf{E}_I^{+i}(t)U_i + \mathbf{E}_I^{+r}(t)U_r + \mathbf{E}_I^{+d}(t) + \mathbf{E}_I^{+sd}(t) \quad (1)$$

where the spatial unit step functions U_i and U_r are unity on the lit side of the incident and reflection shadow boundaries, respectively, and zero otherwise. The TD-UTD incident and reflected GO fields are denoted by \mathbf{E}_I^{+i} and \mathbf{E}_I^{+r} , respectively. The first order TD-UTD edge diffracted is \mathbf{E}_I^{+d} , and the higher order edge diffracted field, which is referred to as the slope edge diffracted field is denoted here by \mathbf{E}_I^{+sd} . The terms in (1) other than the slope diffraction contribution are discussed in detail in [1] and will not be repeated here. Primary attention in this section will therefore be focused on the development of only the slope diffracted contribution. Before proceeding to the formulation of the slope diffracted field, it is noted that the temporal behavior of the time impulsive incident wave is denoted by the analytic delta function $\delta^+(t - s^i/c)$ as done previously for the development of $\mathbf{E}_I^{+d}(t)$ in [1]. Here s^i denotes the distance from a reference point on the incident ray to any point on the curved wege (e.g. point of incidence on the edge, or point of reflection on a curved face of the wedge, etc. [1]). Also, the solution to a general transient incident pulse can be obtained by convolving it with the TD-UTD impulse response as indicated previously in [1]. It is shown in [1] that the convolution can be expressed essentially in closed form for many practical pulse shapes if one employs the ATT, together with a highly compact and simple expansion for the general pulse in which the frequency domain form of the expansion functions is a complex exponential; the latter applies to slope diffraction as well. Furthermore, it is noted that in addition to edge diffracted rays that are launched directly into space external to the curved wedge faces via diffraction of the incident wavefront by the edge, there are also surface

diffracted rays, and whispering gallery rays, launched on convex, and concave wedge faces, respectively, via edge diffraction. The latter edge excited surface ray and whispering gallery effects as well as their reciprocal cases are not considered in the present development.

The slope diffracted field for a curved wedge is given in the frequency (ω) domain by

$$\tilde{\mathbf{E}}^{sd} = \hat{\beta}_0 \tilde{E}_{\beta_0}^{sd} + \hat{\phi} \tilde{E}_{\phi}^{sd} \tag{2}$$

where [9,10]

$$\begin{bmatrix} \tilde{E}_{\beta_0}^{sd} \\ \tilde{E}_{\phi}^{sd} \end{bmatrix} = \left\{ \begin{array}{l} -\tilde{D}^{si} \frac{\partial \tilde{E}_{\beta_0}^i}{\partial n^i} - \tilde{D}_s^{sr} \frac{\partial \tilde{E}_{\beta_0}^r}{\partial n^r} \\ -\tilde{D}^{si} \frac{\partial \tilde{E}_{\phi'}^i}{\partial n^i} - \tilde{D}_h^{sr} \frac{\partial \tilde{E}_{\phi'}^r}{\partial n^r} \end{array} \right\} |A_d(s^d)| j^{n_d} e^{-jk s^d}. \tag{3}$$

The unit vectors $\hat{\beta}_0$ and $\hat{\phi}$ are defined with respect to the plane of diffraction containing the diffracted ray and the edge tangent at the point of diffraction Q_E on the edge as shown in Figure 1; these unit vectors are identical to those utilized in [1] for describing the polarization of the ordinary (as opposed to slope) diffracted field. In particular, $\hat{\beta}_0$ lies in this edge fixed plane of diffraction while $\hat{\phi}_0$ is perpendicular to that plane; furthermore, both these unit vectors are transverse to the diffracted ray whose direction is \hat{s}^d in Figure 1. Also $\hat{\beta}_0 \times \hat{\phi}_0 = \hat{s}^d$. The polarization of the incident or reflected ray fields are like wise expressed, for the representation of the slope diffracted fields, in terms of the unit vectors placed in the edge fixed planes of incidence or reflection defined by the incident or reflected ray and the edge tangent, respectively. The incident and reflected ray directions at Q_E are \hat{s}^i and \hat{s}^r . The unit vectors $(\hat{\beta}'_0, \hat{\phi}')$ and $(\hat{\beta}'_r, \hat{\phi}'_r)$ for the ray incident at Q_E and the ray reflected from Q_E , respectively, play the same role as does $(\hat{\beta}_0, \hat{\phi})$ for the diffracted ray. The extra superscript s on the diffracted field and the slope diffraction coefficients $\tilde{D}^{si}, \tilde{D}_r^{sr}$ and \tilde{D}_h^{sr} indicates slope diffraction, instead of ordinary diffraction which is studied in [1]. The spread factor $|A_d(s^d)|$ of the diffracted ray is defined in [1]; it is assumed here that this diffracted ray spread factor is not rapidly varying. The only rapid variation is assumed to be in the incident and hence the reflected field as well in the \hat{n}^i and \hat{n}^r directions, where \hat{n}^i and \hat{n}^r are normal to the edge fixed planes of incidence and reflection at Q_E , respectively. For a straight wedge, with planar faces, the above expression in (3) simplifies to

$$\begin{bmatrix} \tilde{E}_{\beta_0}^{sd} \\ \tilde{E}_{\phi}^{sd} \end{bmatrix} = \left\{ \begin{array}{l} -\tilde{D}_s^s \frac{\partial \tilde{E}_{\beta_0}^i}{\partial n^i} \\ -\tilde{D}_h^s \frac{\partial \tilde{E}_{\phi'}^r}{\partial n^r} \end{array} \right\} |A_d(s^d)| j^{n_d} e^{-jk s^d} \tag{4}$$

where $\tilde{D}_s^s \equiv \tilde{D}^{si} + \tilde{D}_s^{sr}$ and $\tilde{D}_h^s \equiv \tilde{D}^{si} + \tilde{D}_h^{sr}$. The frequency domain diffraction coefficients in this special case of a straight wedge with plane faces as developed by Hwang and Kouyoumjian are obtained from [9], and those developed by Veruttipong and Kouyoumjian are obtained from [10]. They are summarized separately in appendices A and b, respectively. It is noted that the frequency domain results in [9,10] for the straight wedge are generalized to the curved wedge with curved faces using the principle of locality of high frequency fields [14-16] to arrive at the result in (3). The APT applied to (3) yields the analytic time representation for the slope diffracted fields corresponding to (3) as

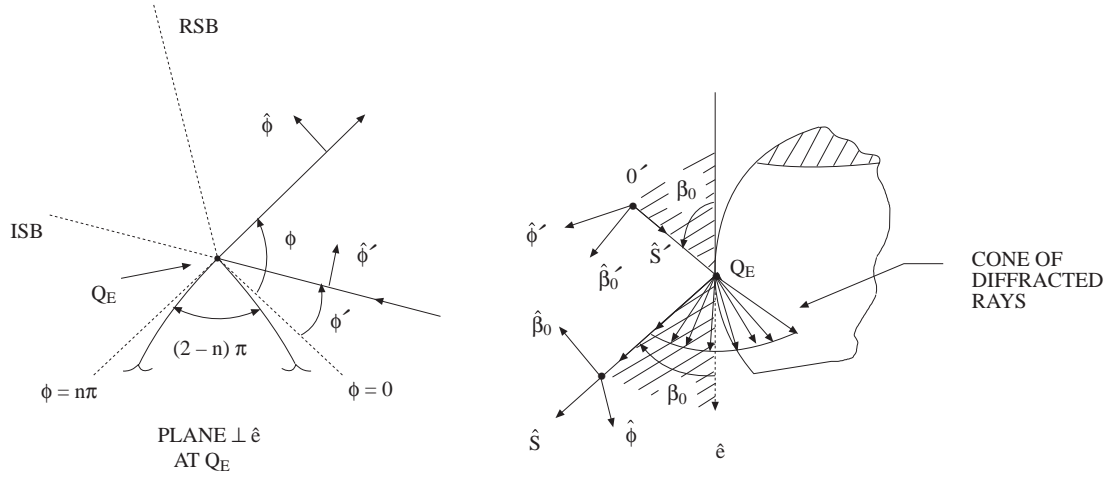


Figure 1. Coordinate systems for the TD-UTD dyadic diffraction coefficient.

$$\begin{bmatrix} \overset{+}{E}_{\beta_0}^{sd}(t) \\ \overset{+}{E}_{\phi}^{sd}(t) \end{bmatrix} = \frac{1}{2} \left\{ \begin{array}{l} -\overset{+}{D}^{si}(t) * \frac{\partial \overset{+}{E}_{\beta_0'}(t)}{\partial n^i} - \overset{+}{D}^{sr}(t) * \frac{\partial \overset{+}{E}_{\beta_0'}(t)}{\partial n^r} \\ -\overset{+}{D}^{si}(t) * \frac{\partial \overset{+}{E}_{\phi'}(t)}{\partial n^i} - \overset{+}{D}^{sr}(t) * \frac{\partial \overset{+}{E}_{\phi'}(t)}{\partial n^r} \end{array} \right\} |A_d(s^d)| \quad (5)$$

in which $*$ denotes an ATT based TD convolution. The analytic impulse response is obtained from (5) by letting the incident field (and hence also the reflected field) in (5) be impulsive in time. In the case of the impulse response which is of primary interest, the TD convolution in (5) becomes simple to evaluate in closed form requiring the variable t in the slope diffraction coefficients in (5) to be replaced by τ_d where $\tau_d = t - \frac{s^i}{c} - \frac{s^d}{c}$, in which s^i and s^d are the distances from the source and observer to Q_E , respectively. As stated earlier, once the impulse response is obtained, the response to any other realistic pulsed excitation can then be obtained by convolving it with the impulse response.

The slope diffraction coefficients, which have been generalized to the curved wedge case, are given separately below in part (a) for the Hwang and Kouyoumjian [9] case (denoted as ‘‘Hwa’’ case), and in part (b) for the Veruttipong and Kouyoumjian [10] case (denoted as the ‘‘Ver’’ case), respectively.

2.1. Analytic TD version of the ‘‘Hwa’’ based curved wedge slope diffraction coefficients

For the ‘‘Hwa’’ case, the $\overset{+}{D}^{si}$ and $\overset{+}{D}_{s,h}^{sr}$ in (3) are given by generalizing the straight wedge results of Appendix B to the curved wedge as follows,

$$\overset{+}{D}^{si}(t) = \frac{-1}{4n^2\sqrt{2\pi}\sin^2\beta_0} \left[C_1 \overset{+}{F}_s(x_1, t) - C_2 \overset{+}{F}_s(x_2, t) \right] \quad (6)$$

$$\overset{+}{D}_{s,h}^{sr}(t) = \frac{\mp 1}{4n^2\sqrt{2\pi}\sin^2\beta_0} \left[C_3 \overset{+}{F}_s(x_3, t) - C_4 \overset{+}{F}_s(x_4, t) \right] \quad (7)$$

with $F_s^+(x_m, t)$ specifically as in (B.3) of appendix B. For the real time case one lets $Im(t) = 0$ in (B.3). Also, the coefficients C_1 , C_2 , C_3 and C_4 are defined for the curved wedge case by

$$C_1 = \csc^2 \left(\frac{\pi + \beta^-}{2n} \right) \tag{8}$$

$$C_2 = \csc^2 \left(\frac{\pi - \beta^-}{2n} \right) \tag{9}$$

$$C_3 = \csc^2 \left(\frac{\pi + \beta^+}{2n} \right) \tag{10}$$

$$C_4 = \csc^2 \left(\frac{\pi - \beta^+}{2n} \right) \tag{11}$$

2.2. Analytic TD version of the “Ver” based curved wedge slope diffraction coefficients

In the “Ver” case, the TD curved wedge coefficients are given as follows,

$$D^{+si}(t) = \frac{-1}{4n^2 \sqrt{2\pi} \sin^2 \beta_0} \sum_{m=1}^2 A_m F_{vs}^+(x_m, t) + B_m F_s^+(x_m, t) \tag{12}$$

$$D^{+sr}(t) = \frac{\mp 1}{4n^2 \sqrt{2\pi} \sin^2 \beta_0} \sum_{m=3}^4 A_m F_{vs}^+(x_m, t) + B_m F_s^+(x_m, t) \tag{13}$$

where $F_s^+(x_m, t)$ and $F_{vs}^+(x_m, t)$ are given specifically as in (B.3) and (B.9), respectively, of Appendix B. Again, the real time solution is obtained by letting $Im(t) = 0$ in the ATT representation.

Although slope diffraction coefficients given above have been generalized to the curved wedge, they may not fully compensate the discontinuous spatial derivative of the reflected field in both, frequency and time domains, when the reflecting wedge face is curved. Nevertheless, the slope diffracted field presented here will provide a good approximation in many practical situations. For a more complete discussion on this aspect, one is referred to the thesis by Zheng [17].

3. Numerical Examples

In [1], a description is provided which allows one to conveniently and efficiently convolve the impulse response with a relatively general transient excitation pulse to obtain a response to the latter more practical situation. The basic procedure in such a convolution procedure is to expand the temporal part, $F_0^i(t)$, of the general excitation pulse in terms of analytic functions given below:

$$F_0^i(t) = \text{Re} \left[\overset{+}{F}_0^i(t) \right] = \text{Re} \left[\frac{j}{\pi} \sum_{n=1}^N \frac{A_n}{t + j\alpha_n} \right] \quad (14)$$

The expansion functions have a simple frequency response in terms of complex exponentials since $\tilde{F}_0^i(\omega)$ which is the Fourier transform of $F_0^i(t)$ can be expressed as

$$\tilde{F}_0^i(\omega) = \sum_{n=1}^N A_n e^{-\alpha_n \omega}, \quad \omega \geq 0 \quad (15)$$

where A_n and α_n are generally complex and must be found by matching the expansions of either (14) or (15), to the time, or frequency behavior of the excitation pulse, respectively. Now, if one denotes $\overset{+}{E}_I^{UTD}(t)$ as the impulse response as indicated in (1), then using the ATT convolution property [1] together with (14) allows one to obtain the response to the general pulsed excitation as

$$\overset{+}{E}^{UTD}(t) = \frac{1}{2} \overset{+}{F}_0^i(t) * \overset{+}{E}_I^{UTD}(t) \quad (16)$$

$$= \sum_{n=1}^N A_n \overset{+}{E}_I^{UTD}(t + j\alpha_n) \quad (17)$$

Of course, the real time response $\tilde{E}^{UTD}(t)$ is the real part of (16) with $\text{Im}(t) = 0$. The analytic function resulting from the convolution in (16) is analytic on the real time axis provided $\text{Re}(\alpha_n) > 0$ for all n , therefore the result $\tilde{E}^{UTD}(t)$ is finite and well behaved. The idea here is that for many practical situations only a handful of terms may be necessary in the expansion of (14) and hence also in the final result of (17) thus making convolution highly efficient.

While the TD slope diffraction by a general curved wedge, excited by a general astigmatic pulsed wave illumination with rapid spatial amplitude variation, can be treated using the impulse response expressions obtained in Section 2, only the case of impulsive spherical wave with rapid spatial variation near the edge of a straight wedge is considered in the numerical calculations shown below. The reason for the latter is that an exact TD solution for a straight wedge subjected to an impulsive illumination from an infinitesimal current element obtained by Felsen [13] is readily available for comparison to assess the accuracy of the TD-UTD slope diffraction solution. The infinitesimal current element is chosen to have a step function behavior in time so that it generates, to first order, an impulsive spherical wave with rapid spatial variation near the pattern null of the current element. For an infinitesimal electric current element, the TD-UTD results and the corresponding reference solutions are shown in Figure 2. The case of a magnetic current excitation is depicted in Figure 3. It is noted from the numerical results that the ‘‘Ver’’ based TD-UTD slope diffraction solution is more accurate for early time; whereas, the ‘‘Hwa’’ solution is more accurate for intermediate to late times as expected from the comments in Appendix A, which briefly discusses how the ‘‘Hwa’’ and ‘‘Ver’’ solutions are constructed in the frequency domain. Also, there is excellent agreement for an observer near the shadow boundary and far away from the shadow boundary, thereby leading confidence in the TD-UTD for practical applications.

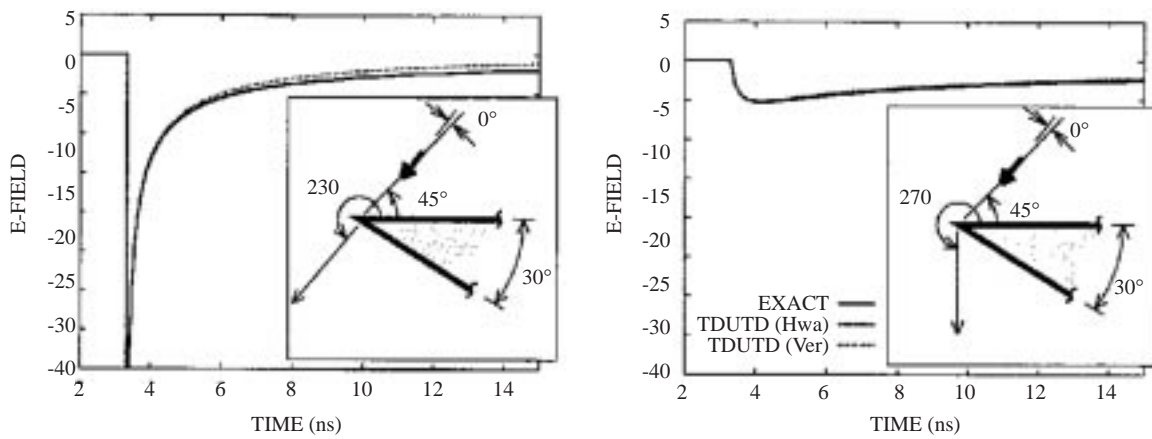


Figure 2. The two versions of the TD-UTD slope diffraction are compared with an exact result. The infinitesimal electric current has a unit step time behavior, which approximately illuminates the wedge with an impulsive spherical wave.

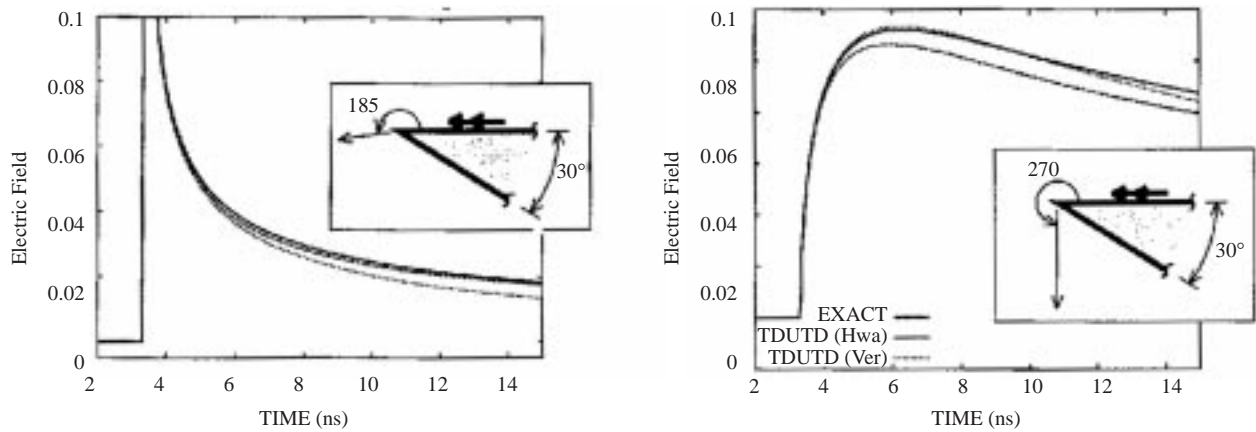


Figure 3. The two versions of the TD-UTD slope diffraction are compared with an exact result. The infinitesimal magnetic current has a unit step time behavior, which approximately illuminates the wedge with an impulsive spherical wave.

Appendix A : Frequency Domain Slope Diffraction Coefficients

The UTD based slope diffraction coefficients by Hwang and Kouyoumjian [9] and by Veruttipong and Kouyoumjian [10] respectively, which are given in the frequency domain for a straight wedge, are summarized here. For the sake of brevity the aforementioned diffraction coefficients will be referred to as “Hwa” and “Ver”, respectively as indicated earlier. The “Hwa” slope diffraction coefficients are obtained in [9] by taking the derivative with respect to ϕ' of the exact spectral integral form of the ordinary wedge diffraction coefficients. The operations of differentiation and integration are interchanged and the resulting spectral integral is then evaluated asymptotically leading to the final result. The “Ver” slope diffraction coefficients on the other hand are obtained by directly differentiating the asymptotic approximation of the spectral integral, which is evaluated first.

A.1 “Hwa” slope diffraction coefficients

The “Hwa” slope diffraction coefficients for a straight wedge, are given as [9]

$$D_{s,h}^s = \frac{-1}{4n^2\sqrt{2\pi}\sin^2\beta_0} \sum_{m=1}^4 C_m^{s,h} \tilde{F}_s(x_m, \omega) \quad (\text{A.1})$$

where

$$C_1^{s,h} = +\csc^2 [(\pi + \beta^-)/2n] \quad (\text{A.2})$$

$$C_2^{s,h} = -\csc^2 [(\pi - \beta^-)/2n] \quad (\text{A.3})$$

$$C_3^{s,h} = \pm \csc^2 [(\pi + \beta^+)/2n] \quad (\text{A.4})$$

$$C_4^{s,h} = \mp \csc^2 [(\pi - \beta^+)/2n] \quad (\text{A.5})$$

and

$$\tilde{F}_s(x_m, \omega) = 2x_m \left[\frac{\sqrt{c}}{\sqrt{j\omega}} - \tilde{F}(x_m, \omega) \right] \quad (\text{A.6})$$

with

$$\tilde{F}(x_m, \omega) = \frac{\sqrt{c}}{\sqrt{j\omega}} \tilde{F}_{tr} \left(\frac{\omega x_m}{c} \right) \quad (\text{A.7})$$

where $\tilde{F}_{tr}(z)$ is the UTD transition function for ordinary wedge diffraction defined by [14]

$$\tilde{F}_{tr}(z) = 2j\sqrt{z}e^{jz} \int_{\sqrt{z}}^{\infty} e^{-j\tau^2} d\tau \quad (\text{A.8})$$

The $\tilde{F}(x_m, \omega)$ function of (A.7) can also be expressed as

$$\tilde{F}(x_m, \omega) = \sqrt{\pi x_m} e^{j\omega x_m/c} \operatorname{erfc} \left(\sqrt{\frac{j\omega x_m}{c}} \right) \quad (\text{A.9})$$

where erfc is the complementary error function given by:

$$\operatorname{erfc}(z) = \frac{2}{\sqrt{\pi}} \int_z^{\infty} e^{-t^2} dt \quad (\text{A.10})$$

The x_m in (A.1) for the straight-wedge are defined as follows [14]:

$$x_1 = La^+(\beta^-) \tag{A.11}$$

$$x_2 = La^-(\beta^-) \tag{A.12}$$

$$x_3 = La^+(\beta^+) \tag{A.13}$$

$$x_4 = La^-(\beta^+) \tag{A.14}$$

In (A.10)-(A.13), $a^\pm(\beta) = 2 \cos^2 [(2n\pi N^\pm - \beta)/2]$ and N^\pm is an integer which most nearly satisfies $(-\beta + 2n\pi N^\pm = \pm\pi)$. All of the above parameters including the L parameter for the straight wedge are available in [14,15].

A.2 “Ver” slope diffraction coefficients

The “Ver” slope diffraction coefficients for a straight wedge are given as [10].

$$D_{s,h}^s = \frac{-1}{4n^2 \sqrt{2\pi} \sin^2 \beta_0} \begin{bmatrix} +A_1 \tilde{F}_{vs}(x_1, \omega) + B_1 \tilde{F}_s(x_1, \omega) \\ -A_2 \tilde{F}_{vs}(x_2, \omega) - B_2 \tilde{F}_s(x_2, \omega) \\ \pm A_3 \tilde{F}_{vs}(x_3, \omega) \pm B_3 \tilde{F}_s(x_3, \omega) \\ \mp A_4 \tilde{F}_{vs}(x_4, \omega) \mp B_4 \tilde{F}_s(x_4, \omega) \end{bmatrix} \tag{A.15}$$

where

$$A_1 = \csc^2((\pi + \beta^-)/2n) - B_1 \tag{A.16}$$

$$A_2 = \csc^2((\pi - \beta^-)/2n) - B_2 \tag{A.17}$$

$$A_3 = \csc^2((\pi + \beta^+)/2n) - B_3 \tag{A.18}$$

$$A_4 = \csc^2((\pi - \beta^+)/2n) - B_4 \tag{A.19}$$

and

$$B_1 = + \frac{n \dot{a}^+(\beta^-)}{a^+(\beta^-)} \cot((\pi + \beta^-)/(2n)) \tag{A.20}$$

$$B_2 = -\frac{n\dot{a}^-(\beta^-)}{a^-(\beta^-)} \cot((\pi - \beta^-)/(2n)) \quad (\text{A.21})$$

$$B_3 = +\frac{n\dot{a}^+(\beta^+)}{a^+(\beta^+)} \cot((\pi + \beta^+)/(2n)) \quad (\text{A.22})$$

$$B_4 = -\frac{n\dot{a}^-(\beta^+)}{a^-(\beta^+)} \cot((\pi - \beta^+)/(2n)) \quad (\text{A.23})$$

All the parameters occurring in the “Ver” slope diffraction coefficients are the same as in the “Hwa” solution and have been defined above. The only other transition function, \tilde{F}_{vs} , present in the “Ver” solution is defined as

$$\tilde{F}_{vs}(x_m, \omega) = \frac{c^{3/2}}{j\omega\sqrt{j\omega}} \tilde{F}_{tr}\left(\frac{x_m\omega}{c}\right) \quad (\text{A.24})$$

and \tilde{F}_{tr} is the one defined in (A.8). This function and $\tilde{F}_{vs}(x_m, \omega)$ of (A.24) can also be alternatively expressed as:

$$\tilde{F}_{vs}(x_m, \omega) = \frac{c}{j\omega} \sqrt{\pi x_m} e^{j\omega x_m/c} \text{erfc}\left(\sqrt{\frac{j\omega x_m}{c}}\right) \quad (\text{A.25})$$

Notice also that

$$\tilde{F}_{vs}(x_m, \omega) = \frac{c}{j\omega} \tilde{F}(x_m, \omega) \quad (\text{A.26})$$

which is a relationship useful for developing the TD version of the “Ver” slope diffraction coefficients.

Appendix B : Analytic Time Transform (ATT) of the Frequency Slope Diffraction Coefficients

In this appendix, the ATT of the “Hwa” and “Ver” frequency domain slope diffraction coefficients of [9,10], described in Appendix A, are developed. The “Hwa” and the “Ver” cases are treated separately in parts B.1 and B.2, respectively.

B.1 ATT of the “Hwa” frequency domain slope diffraction coefficients

From (A.1), one may write the analytic time function representation of the “Hwa” slope diffraction coefficients as

$$D_{s,h}^+(t) = \frac{-1}{4n^2\sqrt{2\pi}\sin^2\beta_0} \sum_{m=1}^4 C_m^{s,h} F_s^+(x_m, t) \quad (\text{B.1})$$

in which $\overset{+}{F}_s(x_m, t)$ is the ATT of $\tilde{F}(x_m, \omega)$ given by [8].

$$\overset{+}{F}_s(x_m, t) = 2x_m \left[\frac{e^{-j\pi/4}\sqrt{c}}{\sqrt{\pi}\sqrt{-jt}} + \frac{j\sqrt{-x_m/\pi}}{\sqrt{-jt}(\sqrt{-jt} + e^{-j\pi/4}\sqrt{-x_m/c})} \right] \tag{B.2}$$

The above expression in (B.2) can be further simplified to yield

$$\overset{+}{F}_s(x_m, t) = \sqrt{\frac{c}{\pi}} \frac{2x_m e^{-j\pi/4}}{\sqrt{-jt} + e^{-j\pi/4}\sqrt{-x_m/c}} \tag{B.3}$$

B.2 ATT of the ‘‘Ver’’ frequency domain slope diffraction coefficients

From (A.15), one may obtain the ATT of the ‘‘Ver’’ slope diffraction coefficients by simply obtaining the ATT of the functions \tilde{F}_{vs} and \tilde{F}_s only since all other quantities in (A.15) besides these two functions are frequency independent. The ATT of \tilde{F}_s has been given earlier in B.1 for the ‘‘Hwa’’ case. It now remains to provide the ATT of \tilde{F}_{vs} . However, from (A.26) the \tilde{F}_{vs} can be expressed in terms of \tilde{F} which has the following ATT

$$\overset{+}{F}(x_m, t) = \frac{-j\sqrt{-x_m/\pi}}{\sqrt{-jt}(\sqrt{-jt} + e^{-j\pi/4}\sqrt{-x_m/c})} = \frac{x_m}{\sqrt{\pi c}} \frac{1}{\sqrt{t}(t + x_m/c)} + j \frac{\sqrt{x_m/\pi}}{t + x_m/c} \tag{B.4}$$

for $Imt \geq 0$ where

$$\sqrt{-x_m} = \begin{cases} j\sqrt{x_m}, & x_m > 0 \\ \sqrt{-x_m}, & x_m < 0 \end{cases} \tag{B.5}$$

and $Re(\sqrt{-jt}) > 0$.

Next, the following property of the ATT is utilized to obtain the ATT of \tilde{F}_{vs} [4,8]

$$\frac{1}{j\omega} \tilde{H}(\omega) \overset{A}{\longleftrightarrow} \overset{+}{H}^{(-1)}(t) + C_0 \tag{B.6}$$

in which $\overset{+}{H}^{(-1)}(t)$ is the primitive or anti-derivative of $\overset{+}{H}(t)$ and C_0 is a constant to be determined. Using (B.6), the ATT of \tilde{F}_{vs} is

$$\begin{aligned} \overset{+}{F}_{vs}(x_m, t) &= jc\sqrt{\frac{x_m}{\pi}} \left[\ln \left(\frac{\sqrt{t} + j\sqrt{x_m/c}}{\sqrt{t} - j\sqrt{x_m/c}} \right) + \ln(t + x_m/c) \right] + C_0 \\ &= j2c\sqrt{\frac{x_m}{\pi}} \ln \left(\sqrt{t} + j\sqrt{x_m/c} \right) + C_0 \\ &= j2c\sqrt{\frac{x_m}{\pi}} \left[\ln \left| \sqrt{t} + j\sqrt{x_m/c} \right| + j \arg \left(\sqrt{t} + j\sqrt{x_m/c} \right) \right] + C_0 \end{aligned} \tag{B.7}$$

where $\arg(z)$ denotes the argument of the complex number z . Here C_0 is chosen that $F_{vs}^+ = 0$ when $t = 0$ (with $x_m > 0$); such a condition appears reasonable since it is true in general that in the frequency domain,

$$\lim_{\omega \rightarrow \infty} j\omega \tilde{H}(\omega) = \lim_{(-jt) \rightarrow 0} \left[-j\dot{H}^+(t) - jt \frac{\partial}{\partial t} \dot{H}^+(t) \right]$$

and

$$\lim_{\omega \rightarrow \infty} j\omega \tilde{F}_{vs}(x_m, \omega) = 0 \quad (\text{B.8})$$

Thus

$$F_{vs}^+(x_m, t) = jc \sqrt{\frac{x_m}{\pi}} \left[\ln \left| \frac{\sqrt{t} + j\sqrt{x_m/c}}{\sqrt{x_m/c}} \right| + \arg \left(\sqrt{t} + j\sqrt{x_m/c} \right) - j\frac{\pi}{2} \right]$$

A more convenient form for calculations utilizes $\sqrt{x_m} = -j\sqrt{-x_m}$ because $\frac{-\pi}{2} < \arg(-x_m) < \frac{3\pi}{2}$ and $\sqrt{t} = e^{j\frac{\pi}{4}}\sqrt{-jt}$ (since $-\pi < \arg(-jt) < \pi$) to obtain

$$F_{vs}^+(x_m, t) = \frac{2c\sqrt{-x_m}}{\sqrt{\pi}} \left[\ln \left| \frac{e^{j\pi/4}\sqrt{-jct} + \sqrt{-x_m}}{\sqrt{-x_m}} \right| + j \arg \left(e^{j\pi/4}\sqrt{-jct} + \sqrt{-x_m} \right) - j\frac{\pi}{2} \right] \quad (\text{B.9})$$

Acknowledgement

The final preparation of this manuscript was supported in part by a subcontract to The Ohio State University, that is associated with a parent contract # F49620-01-C-0045 from the Air Force Office of Scientific Research.

References

- [1] P. R. Rousseau and P.H. Pathak, "Time-Domain Uniform Geometrical Theory of Diffraction for a Curved Wedge," *IEEE Trans. AP-43*, No. 12, December. 1995, pp. 1375-1382.
- [2] E. Heyman and L. B. Felsen, "Weakly Dispersive Spectral Theory of Transients (STT), Part I: Formulation and Interpretation," *IEEE Trans. AP*, vol. AP-35, pp. 80-86, January 1987.
- [3] E. Heyman and L. B. Felsen, "Weakly Dispersive Spectral Theory of Transients (STT), Part II: Evaluation of the Spectral Integral," *IEEE Trans. AP*, vol. AP-35, pp. 574-480, May 1987.
- [4] E. Heyman, "Weakly Dispersive Spectral Theory of Transients (STT), Part III: Applications," *IEEE Trans. AP*, vol. AP-35, pp. 1258-1987, November 1987.
- [5] E. Heyman and R. Iaconescu, "Pulsed Field Diffraction by a Perfectly Conducting Wedge: Local Scattering Models," *IEEE Trans. AP*, vol. 43, pp. 519-528, May 1995.
- [6] R. Iaconescu and E. Heyman, "Pulsed Field Diffraction by a Perfectly Conducting Wedge: Exact Solution," *IEEE Trans. AP*, vol. 42, pp.1377-1385, October 1994.

- [7] R. Iaconescu and E. Heyman, "Pulsed Field Diffraction by a Perfectly Conducting Wedge: A Spectral Theory of Transients Analysis," *IEEE Trans. AP*, vol. 42, pp., 781-789, June 1994.
- [8] P. R. Rousseau, "Time Domain Version of the Uniform Geometrical Theory of Diffraction," Ph.D. Dissertation, Dept. of Electrical Engineering, The Ohio State University, Columbus, Ohio, 1995.
- [9] Y. M. Hwang and R. G. Kouyoumjian, "A Dyadic Diffraction Coefficient for an Electromagnetic Wave Which is Rapidly Varying at an Edge," USNC-URSI, 1974. Presented at the USNC-URSI Annual Meeting, Boulder, CO, October, 1974.
- [10] T. Veruttipong. "Diffraction at Edges and Convex Surfaces Illuminated by Fields with a Rapid Spatial Variation," Ph.D. Dissertation, Dept. of Electrical Engineering, The Ohio State University, Columbus, OH 1982.
- [11] O. M. Buyukdura, "GTD Solution With Higher Order Terms to the Diffraction by an Edge: Towards a Uniform Solution," *IEE Proc. Microw., Antennas, Propag.*, vol. 143, pp. 43-50, 1996.
- [12] O. Breinbjerg, "A Slope Diffraction Coupling Effect," *Electromagnetics* (special issue on the centennial of Sommerfeld's diffraction problem), vol. 18, No. 2, pp. 179-206, March 1998.
- [13] L. B. Felsen and N. Marcuvitz, *Radiation and Scattering of Waves*. Englewood Cliffs, NJ: Prentice Hall, 1973.
- [14] R. G. Kouyoumjian and P.H. Pathak, "A Uniform Geometrical Theory of Diffraction for an Edge in a Perfectly Conducting Surface," *Proc. IEEE*, vol. 62, pp. 1448-1461, November 1974
- [15] P. H. Pathak, "Techniques for High Frequency Problems," *Antenna Handbook: Theory, Application and Design* (Y.T. Lo and S.W. Lee, eds.), ch. 4, Van Nostrand Reinhold Company, 1988.
- [16] P. H. Pathak, "High Frequency Techniques for Antenna Analysis," *Proc. IEEE*, vol. 80, pp. 44-65, January 1992.
- [17] D. Zheng, "A Modified Slope Diffraction for a Curved Wedge or Screen," M.S. Thesis, Dept. of Electrical Engineering, The Ohio State University, Columbus, Ohio, 1985.